Vol 4, 1 (2018) 1-8

Contents lists available at Article URL

KKU Journal of Basic and Applied Sciences

Journal homepage: jbas.kku.edu.sa

Heat and Mass Transfer in Membrane Based Enthalpy Exchanger Applied to Desalination of Seawater

S. Asiri[a], F. Maiz[a,b,*], and R. Chouikh[a,b]

[a] King Khalid University, Faculty of Science, Physics Department P.O. Box 9004 Abha, Saudi Arabia
[b] Thermal Process Laboratory Research and Technologies Centre of Energy, BP 95, 2050 Hammam-lif, Tunisia.

Received: May 2018 / Revised: July 2018 / Accepted: September 2018 / Published: 25 December 2018

Abstract: This study deals with a two-dimensional numerical model of the coupled transfers of heat and mass in a counter-flow enthalpy exchanger. This work involves the use of a control-volume method and solves the energy and mass equations in the membrane and channels. The effect of operating parameters such as the flow rates, temperatures concentrations and on the performance of the considered exchanger is also investigated. The obtained numerical results are compared with those of literature and the agreement is satisfactory.

Keywords: Heat and mass transfer, Liquid desiccant, Membrane enthalpy exchanger, Numerical simulation

1. INTRODUCTION

Fresh water constitute one of the most important topics on the international environment. In this context, solar desalination systems using humidification dehumidification process is a promising technology in the future.

Humidification-dehumidification desalination is an imitation version of the natural water cycle, where water is evaporated from the oceans by the sun and condenses into fresh water precipitation, which returns to earth and can be used for drinking. The Sun, which is the driving force of the water cycle, heats water in oceans and sea sand then, water evaporates as water vapor into the air.

Most of the energy recovery devices in the market are limited to recover only sensible heat. However, with enthalpy exchanger, the reduction of the energy consumption can reach 40 % under certain climatic conditions.

The humidifier which is generally a cylindrical vessel, is sprayed by hot water at the top and the air stream flowing upward, is heated and humidified using the energy from the hot water stream. The humidified air is then circulated to the dehumidifier or condenser where it is cooled in a compact heat exchanger by using seawater as the coolant [1]. Humidified air is then cooled to obtain water free of salt by using fresh seawater as a coolant. The seawater is preheated in the process by the humidified air and is further heated in a solar heater before entering the humidifier. The main equipment needed for the relatively new desalination process is: Collectors for heating the salt solution, the Humidifier and the dehumidifier or condenser.

In this context, the membrane-based enthalpy exchangers constitute a promising alternative since there is no requirement to apply hydraulic pressure and it operates at relatively low temperatures with reasonably low capital costs. This leads to utilization of solar energy or waste heat. The humidification process handles the latent load while sensible heating handles the sensible load.

Several studies have been carried out on the experimental and theoretical analysis of the heat and mass transfer process in the membrane-based enthalpy exchanger. One of the early studies is the work of Lof [2] who used triethylene glycol as

the hygroscopic solution in the first liquid desiccant system. The humidification and dehumidification processes have attracted again the interest of several researchers at early 1980s. Several numerical studies

Correspondence:
E-mail: auther@mail.com
Tel: o*******

have been developed to analyze the packed bed desorption humidifiers and to predict the performance of the system: the finite difference approach [3,4], the effectiveness NTU model [5], and the numerical simulation based on fitted algebraic equations [6,7]. However, the one-dimensional finite difference model presented by Factor and Grossman [4] is the commonly used model because it provides the most accurate results. Also, the results of the references [8,9] are in good agreement with the experimental findings.

The moisture transport in desiccant liquid air membrane energy exchangers (DLAMEEs) depends on both membrane design and properties because their ability to recover sensible and latent heat is responsible of its overall efficiency and performance. The transport of vapor water depends on the morphological properties of the membrane such as mass diffusivity, thermal conductivity, thickness and porosity as discussed by [10,11].

Maghaddam et al. [12,13] presented a numerical study of the effects of membrane proprieties such as the vapor diffusion resistance and the air side convective heat transfer coefficient on the effectiveness of the process. The principal results show that the latent effectiveness increases by 11% when vapor diffusion resistance of the membrane decreases from 56 $s.m^{-1}$ to 24 $s.m^{-1}$. Also, by increasing the air convective heat transfer coefficient, the total effectiveness of the process increase by 4%.

Several investigations have been performed on material characteristics used in the in desiccant liquid air membrane energy exchangers such as Nafion [14], cellulose triacetate [15], polyether-polyurethane[16], polyethersulfone [17], PolyVinylidene FluoriDe (PVFD), and polystyrene-sulfonate [18]. The adequate and appropriate liquid desiccants are generally characterized by low vapor pressure, low viscosity and good heat transfer characteristics.

Some researchers have focused their investigations on the flow arrangement effects and the associated geometrical configurations such as co current, counter current and cross flow on the efficiency of the system [19,20].

Some investigations have also noted that the properties of desiccant liquid materials have a strong effect on water vapor transfer through the membrane. In fact, the appropriate choice of the adequate desiccant liquid solution must consider the properties of membranes such as surface vapor pressure, desiccant liquid concentration and its crystallization limit [21]. We can find in the literature several materials that have been used in the desiccant liquid air membrane energy exchangers such as Magnesium Chloride ($MgCl_2$) [22], Lithium Chloride (LiCl) [23], Lithium Bromide (LiBr) [24], and calcium chloride ($CaCl_2$) [25]. Sorption-based processes require only low-grade energy for regeneration of the sorbent materials, thus incurring lower running costs. The Lithium Chloride (LiCl) has a high-saturated pressure, which enhance the transfer of mass end heat in the membrane.

The material considerations and clarification of moisture resistance, the effectiveness correlations for heat and moisture transfer processes and the mass transfer in a cross-flow membrane-based enthalpy exchanger under naturally formed boundary conditions were studied in [26-28].

In recent years, numerous large-scale seawater desalination plants have been built in water-stressed countries to augment available water resources, and construction of new desalination plants is expected to increase in the near future. Despite major advancements in desalination technologies, seawater desalination is still more energy intensive compared to conventional technologies for the treatment of fresh water [29].

The present work studied numerically the coupled heat and mass transfer in a desiccant liquid air membrane energy exchanger as well as the effect of different operating parameters on the performance of the process.

2. MATHEMATICAL MODEL

The enthalpy exchangers which use hydrophobic membranes is composed of several channels and arranged with a stack of square plates leading to a large heat and mass transfer area (Fig. 1).

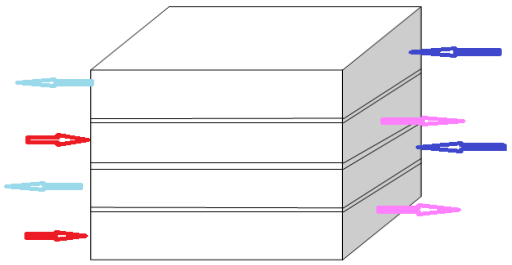

Figure 1: enthalpy exchanger

Air and solution flows are passing alternatively in channels separated by thin membranes. The flows arrangements are in counter flow configuration where the humid air is passing from one direction and the salt solution is passing from the opposite direction of the channels. The used liquid desiccant is the aqueous solution of LiCl.

The driving force of the coupled transfer is a partial vapor pressure difference between the air and solution side which is induced by a temperature gradient

between the two channels. For considerations of symmetry, the calculation domain is composed of a membrane and two neighboring half air and solution ducts (Fig. 2).

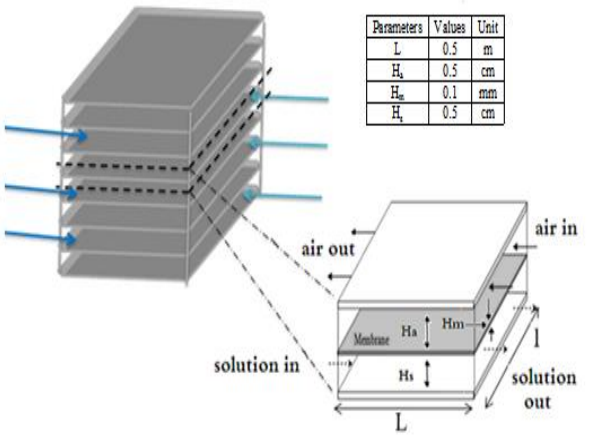

Figure2 : calculation domain

Dashed lines present the boundaries of the considered domain which is shared between the membrane two consecutive half layers.

The principal assumptions used in the mathematical approach are:

- The fluids are Newtonian and incompressible with constant thermal properties.

- The flows are assumed laminar in two channels.

- Because of its weak thickness, water vapor transfer in the membrane is in the thickness direction.

- In the membrane, the coupled transfer in two streams is two dimensional (in x and y directions).

- The heat of sorption is assumed constant and equal to the heat of vaporization.

- The partial vapor pressure in humid air is in balance state with that in the solution.

Taking into account of the precedent assumptions, the dimensionless governing equations for coupled heat and mass transfer through the hydrophobic membrane and channels are written in Cartesian coordinates and in steady state as follows:

The momentum conservation equation in fluid channels is expressed as.

$$\frac{\partial u_i^*}{\partial x_i^*} + \frac{\partial v_i^*}{\partial y_i^*} = 0 \qquad (1)$$

Conservation of momentum equations can be written as:

$$u_i^* \frac{\partial u_i^*}{\partial x_i^*} + v_i^* A_i \frac{\partial u_i^*}{\partial y_i^*} = -\frac{\partial p_i^*}{\partial x_i^*} + \frac{1}{Re_i}\left[\frac{\partial^2 u_i^*}{\partial x_i^{*2}} + A_i \frac{\partial^2 u_i^*}{\partial y_i^{*2}}\right] \quad (2)$$

$$u_i^* \frac{\partial v_i^*}{\partial x_i^*} + v_i^* A_i \frac{\partial v_i^*}{\partial y_i^*} = -\frac{\partial p_i^*}{\partial y_i^*} + \frac{1}{Re_i}\left[\frac{\partial^2 v_i^*}{\partial x_i^{*2}} + A_i \frac{\partial^2 v_i^*}{\partial y_i^{*2}}\right] \quad (3)$$

where $Re_i = \frac{U_{i,inl} H_i}{v_i}$ is the Reynolds number relative to the corresponding moving fluid and Ai is the shape ratio of the corresponding canal.

Also, the heat and mass transfer equations in the two channels are expressed as:

$$u_i^* \frac{\partial \theta_i}{\partial x_i^*} + v_i^* A_i \frac{\partial \theta_i}{\partial y_i^*} = \frac{1}{Re_i Pr_i}\left[\frac{\partial^2 \theta_i}{\partial x_i^{*2}} + A_i \frac{\partial^2 \theta_i}{\partial y_i^{*2}}\right] \quad (4)$$

$$u_i^* \frac{\partial \xi_i}{\partial x_i^*} + v_i^* A_i \frac{\partial \xi_i}{\partial y_i^*} = \frac{1}{Re_i Sc_i}\left[\frac{\partial^2 \xi_i}{\partial x_i^{*2}} + A_i \frac{\partial^2 \xi_i}{\partial y_i^{*2}}\right] \quad (5)$$

where $Pr_i = \frac{v_i}{\alpha}$ and $Sc_i = \frac{v_i}{D}$ denote respectively the Prandtl and Schmidt numbers relative to the corresponding moving fluid.

i designate vapour water for humid air or liquid water for desiccant solution.

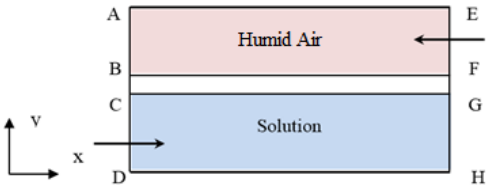

Figure3: boundary conditions

In hydrophobic membrane, heat and moisture transfer in the flow direction are considered negligible due to the small membrane thickness (10^{-4} m) and also to the transversal thermal and mass gradients between the air and solution steams [30]. Then, heat and mass transfer in membrane can be simplified to one-dimensional equation and they are written as:

$$\frac{\partial^2 \theta_a^m}{\partial y_m^2} = 0 \quad (6) \quad \text{and} \quad \frac{\partial^2 \xi_v^m}{\partial y_m^2} = 0 \quad (7)$$

The dimensionless variables are as follows: $x_a^* = \frac{x_a}{H_a}$, $y_a^* = \frac{y_a}{H_a}$, $u_a^* = \frac{u_a}{u_{inl,a}}$, $v_a^* = \frac{v_a}{u_{inl,a}}$, $p_a^* = \frac{p_a}{\rho_a {u_{inl,a}}^2}$, $\theta_a = \frac{T_a - T_{a,inl}}{T_{s,inl} - T_{a,inl}}$, $\theta_a^m = \frac{T_a^m - T_{a,inl}}{T_{s,inl} - T_{a,inl}}$, $\xi_v = \frac{C_v - C_{v,inl}}{C_{w,inl} - C_{v,inl}}$, $\xi_a^m = \frac{C_v^m - C_{v,inl}}{C_{w,inl} - C_{v,inl}}$, $x_s^* = \frac{x_s}{H_s}$, $y_s^* = \frac{y_s}{H_s}$, $u_s^* = \frac{u_s}{u_{inl,s}}$, $v_s^* = \frac{v_s}{u_{inl,s}}$, $p_s^* = \frac{p_s}{\rho_s {u_{inl,a}}^2}$, $\theta_s = \frac{T_s - T_{a,inl}}{T_{s,inl} - T_{a,inl}}$,

$\xi_w = \frac{C_w - C_{w,inl}}{C_{w,out} - C_{w,inl}}$, $x_m^* = \frac{x_m}{H_m}$, $y_m^* = \frac{y_m}{H_m}$, $A_a = \frac{L_a}{H_a}$,

and $A_s = \frac{L_s}{H_s}$

are the shape ratios of the humid air and solution channels.

with La = Ls= Lm = L. L is the length of the considered exchanger.

The used boundary conditions take into account the conservation of the mass and thermal flux densities at the interfaces hydrophobic membrane-channels.

In dimensionless form, the associated boundary conditions, shown in figure 3, are written as follows:

In the air flow channel

Boundary AB: outlet condition for humid air

$x_a^* = A_a\ ,\ 0 \le y_a^* \le 1,\ \frac{\partial \theta_a}{\partial x_a^*} = 0,\ \frac{\partial \xi_v}{\partial x_a^*} = 0, \frac{\partial u_a^*}{\partial x_a^*} = 0$

and $v_a^* = 0$.

Boundary AE: symmetric line of the air channel

$y_a^* = 1\ ,\ 0 \le x_a^* \le A_a,\ \frac{\partial \theta_a}{\partial y_a^*} = 0,\ \frac{\partial \xi_v}{\partial y_a^*} = 0, \frac{\partial u_a^*}{\partial y_a^*} = 0$

and $v_a^* = 0$.

Boundary EF: inlet condition for humid air

$x_a^* = 0\ ,\ 0 \le y_a^* \le 1,\ u_a^* = 1,\ v_a^* = 0, \theta_a = 0$

and $\xi_v = 0$.

Boundary BF: interface air channel-membrane

$y_a^* = 0\ \ 0 \le x_a^* \le A_a,\ \frac{\partial \theta_{a,int}}{\partial y_a} = \left(\frac{\lambda_a^m}{\lambda_a}\right)\left(\frac{H_a}{H_m}\right)\frac{\partial \theta_{a,int}^m}{\partial y_a}$

and $\frac{\partial \xi_{a,int}}{\partial y_a} = (\frac{D_{v,a}^m}{D_{v,a}})(\frac{H_a}{H_m})\frac{\partial \xi_{v,int}^m}{\partial y_a}$.

In the solution flow channel

Boundary CD: Inlet condition for desiccant solution

$x_s^* = 0\ ,\ 0 \le y_s^* \le A_s\ , u_s^* = 1,\ v_s^* = 0, \theta_s = 1$

and $\xi_w = 0$.

Boundary GH: outlet condition for salt solution

$x_s^* = A_s\ ,\ 0 \le y_s^* \le 1,\ \frac{\partial \theta_s}{\partial x_s^*} = 0,\ \frac{\partial \xi_w}{\partial x_s^*} = 0, \frac{\partial u_s^*}{\partial x_s^*} = 0$

and $v_s^* = 0$.

Boundary DH: symmetric line of the solution channel

$y_s^* = 0\ ,\ 0 \le x_s^* \le A_s,\ \frac{\partial \theta_s}{\partial y_s^*} = 0,\ \frac{\partial \xi_w}{\partial y_s^*} = 0, \frac{\partial u_s^*}{\partial y_s^*} = 0$

and $v_s^* = 0$.

- Boundary CG: interface membrane-solution channel

$y_s^* = 1\ ,\ 0 \le x_s^* \le A_s,\ u_s^* = 0, v_s^* = 0,$

$\frac{\partial \theta_s}{\partial y_s^*} = \left(\frac{H_s}{H_m}\right)\left(\frac{\lambda_a^m}{\lambda_s}\right)\frac{\partial \theta_a^m}{\partial y_m^*} + \left(\frac{H_s}{H_m}\right)N^*\frac{\partial \xi_v^m}{\partial y_m^*}L_v\ ,$

$\frac{\partial \xi_w}{\partial y_s^*} = \left(\frac{\rho_a}{\rho_s}\right)\left(\frac{D_{v,a}^m}{D_{w,s}}\right)\left(\frac{H_s}{H_m}\right)\frac{\partial \xi_v}{\partial y_m^*} = 0$

and $N^* = \left(\frac{\rho_a D_{v,a}^m L_v}{\lambda_s}\right)\left(\frac{\Delta C_v}{\Delta T}\right) = \frac{\rho_a D_{v,a}^m \Delta C_v L_v}{\lambda_s \Delta T}$ then

$$N^* = \frac{mass\ transfer\ potential}{heat\ transfer\ potential}$$

N* is the ratio of latent to sensible heat transfer and it is considered as an operating factor.

In the hydrophobic membrane

The vapour pressure at the interfacial temperature plays a crucial role in the exchange of the vapour between the considered solution and the humid air. In fact, the transfer of the water vapor between the solution and the air depends on the relative amplitude of the vapour pressure in the air and at the interface respectively. For high interfacial vapour pressure, the vapour is transferred from the solution to the humid air while for low vapor pressure, the vapor is transferred from the humid air to the solution.

- Boundary BF: interface membrane-air channel

$y_m^* = 1\ ,\ 0 \le x_m \le A_m,\ \theta_a^m = \theta_{a,int},\ \xi_v^m = \xi_{v,int}.$

- Boundary BC: solid boundary

$x_m^* = 0\ ,\ 0 \le y_m^* \le 1, \frac{\partial \theta_a^m}{\partial x_m^*} = 0, \frac{\partial \xi_v^m}{\partial x_m^*} = 0.$

- Boundary FG: solid boundary

$x_m^* = A_m\ ,\ 0 \le y_m^* \le 1, \frac{\partial \theta_a^m}{\partial x_m^*} = 0, \frac{\partial \xi_v^m}{\partial x_m^*} = 0.$

- Boundary CG: interface membrane-solution channel

$y_m^* = 0\ ,\ 0 \le x_m^* \le A_m,\ \theta_a^m = \theta_{s,int},\ \xi_v^m = 1$

with $C_{v,int}^m = f[P_v(T_{s,int}, C_{w,int})]$

$$C_{v,int}^m = \frac{0.62185 P_{v,int}}{P_{atm} - P_{v,int}}$$

P_{atm} is the atmospheric pressure

$P_v(T_{s,int}, C_{w,int})$ which is the vapour pressure at the interfacial temperature, is calculated by using correlations of Conde [31].

$C_{v,int}^m$ is the equilibrium humidity ratio of the air in contact with salt solution at the air-solution interface.

$C_{w,int}$ is the salt solution concentration at the air-solution interface.

$T_{s,int}$ is the salt solution temperature at the air-solution interface.

- Boundary BF: interface membrane-air channel

$y_m^* = 1\ ,\quad 0 \le x_m^* \le A_m\ ,\ \theta_a^m = \theta_{a,int}\ ,\ \xi_{v,int}^m = \xi_{v,int}.$

The performance of the membrane based enthalpy exchanger is evaluated by the efficiency or effectiveness. In fact, the sensible efficiency is written as:

$$\varepsilon_{sen} = \frac{\dot{m}_a Cp_a}{\min(\dot{m}_a Cp_a, \dot{m}_s Cp_s)} \frac{\overline{T_{a,out}} - T_{a,inl}}{T_{s,inl} - T_{a,inl}} \quad (8)$$

The latent efficiency is written as:

$$\varepsilon_{lat} = \frac{\dot{m}_a Cp_a}{\min(\dot{m}_a Cp_a, \dot{m}_s Cp_s)} \frac{\overline{C_{v,out}} - C_{v,in}}{C_{v,int} - C_{v,inl}} \quad (9)$$

$\overline{T_{a,out}}$ and $\overline{C_{a,out}}$ are the space averaged value of the temperature and the specific humidity of the air at the exit of the considered exchanger:

$$\overline{T_{a,out}} = \frac{1}{H_a}\int_0^{H_a} T_{a,out}\, dy \quad (10)$$

and $$\overline{C_{v,out}} = \frac{1}{H_a}\int_0^{H_a} C_{v,out} dy \quad (11)$$

Finally, the humidification mass rate (kgwv/s) is written as:

$$m_{hum} = \dot{m}_a(\overline{C_{v,out}} - C_{v,in}) \quad (12)$$

3. SOLUTION PROCEDURE

The governing equations corresponding to the heat and mass transfers in the membrane and two channels are solved by using the control-volume method developed by Patankar [32]. The most attractive feature of this approach is that the conservation of energy and mass are exactly satisfied. In addition, the mathematical formulations involved in this method do not obscure the physical meaning of each term in the governing equation. First, the calculation domain is divided into a number of non-overlapping control volumes such that there is one control volume surrounding each grid point. Then, each partial differential equation is discretized by integrating it over each control volume by assuming piecewise linear profiles in space. The code uses the SIMPLE algorithm [32] for the pressure and velocity corrections. The obtained system of algebraic equations is solved by using the successive over relaxation method. The solution was considered converged when the relative error between the new and the old values of the considered dependent variable became less than 10-4.

The number of grid points in the x-direction is fixed at 1000 for all compartments of the considered enthalpy exchanger, while the number of grid points in the y-direction varies from 40 for the humid air and desiccant solution channels to 20 for the hydrophobic membrane. The numerical calculation was made by using FORTRAN software. The method employed has been previously successfully utilized and verified for solving more complex problems like the combined heat, mass and electrical charges transfer in a cavity.

4. NUMERICAL RESULTS

Thermal and mass fields in the membrane and both channels in counter-current configuration are presented. The parameters considered are as follows: solution temperature, solution concentration, air temperature, specific humidity of air, and flow velocities of two fluids. Figure 4 presents the mass fields in three domains of the considered exchanger. We remark that the profile of the concentration field is symmetric and parabolic due to the convective effect of the transfers. On the other hand, the iso-concentration are slightly deformed and nearly parallel to the interfaces in the membrane, which indicates that the transfers are dominated by the diffusion phenomena. The effect of convection is seen as the departure of the isotherms from the horizontal.

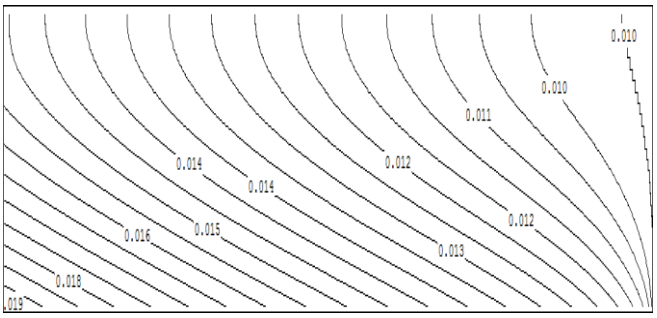

a)

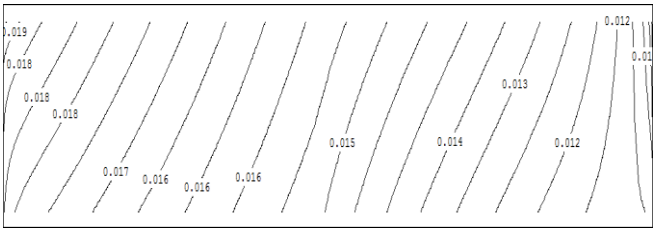

b)

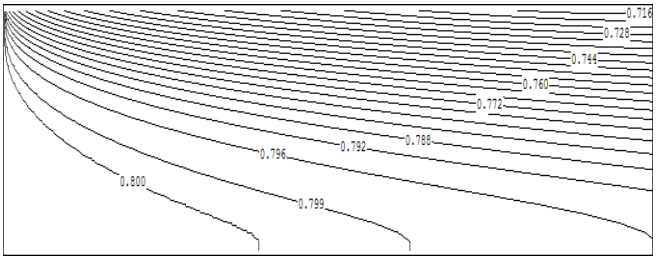

c)

Figure4: Mass concentration fields

a: air channel ; b: membrane ; c: solution channel (Ta,in= 25 °C , Ts,in= 35 °C , ωa,in= 10 g/kg , Cwat,in=80 % , Vs,in= 0,01m/s , Va,in= 0,1m/s)

It is to be noted hear that the same pattern of isotherms is observed because of the similarity between the conservation equations of mass and energy.

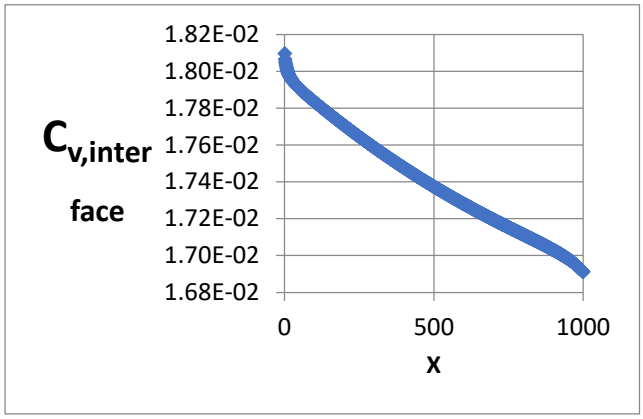

Figure5: Vapour concentration at the interface solution-air (Ta,in= 25 °C , Ts,in= 35 °C , ωa,in= 10 g/kg , Cwat,in=80 % , Vs,in= 0,01m/s , Va,in= 0,1m/s)

Figure 5 presents the concentration of the water vapour at the interface salt solution-humid air. Since the temperature decreases along the channel, we note that the concentration of the water vapour decreases with the extent of the channel accordingly to the correlations of Conde [31], which indicate that the saturated vapour pressure is an increasing function of the solution temperature.

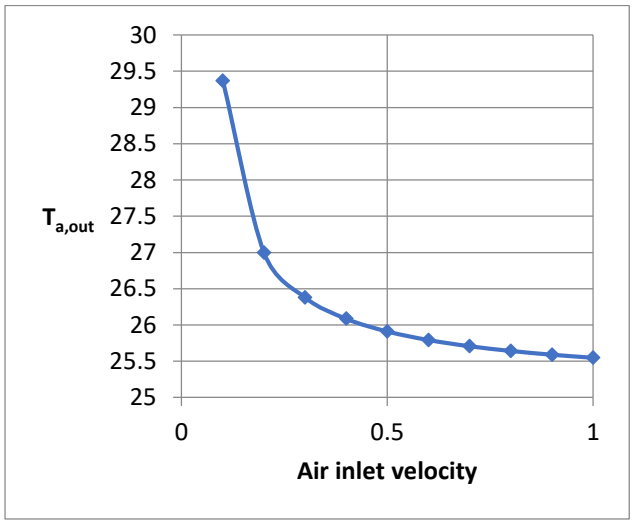

Figure6: Inlet velocity effect of the humid air on the air outlet temperature (Ta,in= 25 °C , Ts,in= 35 °C , ωa,in= 10 g/kg , Cwat,in=80 % , Vs,in= 0,01m/s)

Figure 6 shows the variation of the temperature values at the outlet of the air channel as a function of the air flow velocity for velocities ranging between 0.1 and 1 m.s^{-1}. By increasing the air flow rate, a decrease in the outlet temperature values is observed. The air temperature at the outlet decreases from 29.41 to 25.58 ° C for a variation of the velocity from 0.1 to 1 m s^{-1}. Figure 7 shows the variation of the absolute humidity values of air at the outlet of the air channel as a function of the air flow velocity for velocities ranging between 0.1 m s^{-1} and 1 m s^{-1}. Also, we note a decrease of the outlet absolute humidity of air with increasing air flow velocity.

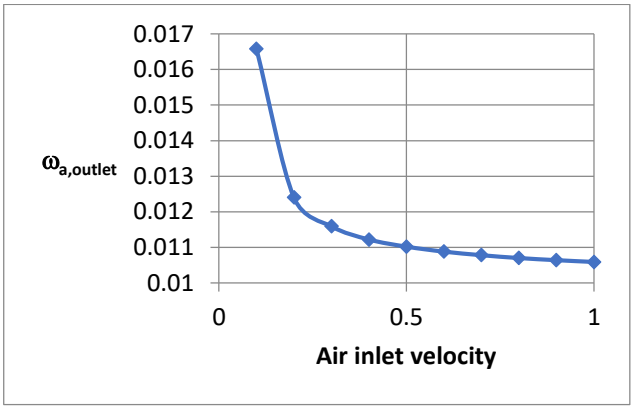

Figure7: Inlet velocity effect of the humid air on the outlet absolute humidity of air (Ta,in= 25 °C , Ts,in= 35 °C , ωa,in= 10 g/kg , Cwat,in=80 % , Vs,in= 0,01m/s)

The results, founds in figures 6 and 7 show that heat and mass transfers in the considered exchanger decrease for relatively high velocity values. However, the temperature and the specific humidity of the humid air greatly decrease until nearly V_{air} = 0.5 m/s , after that the slope of decay becomes weak.

Figure 8 shows the variation of the temperature values at the outlet of the air channel as a function of the solution flow velocity for velocities ranging between 0.01 and 0.1 m.s^{-1}. By increasing the solution flow rate, a weak decrease in the outlet temperature values is observed.

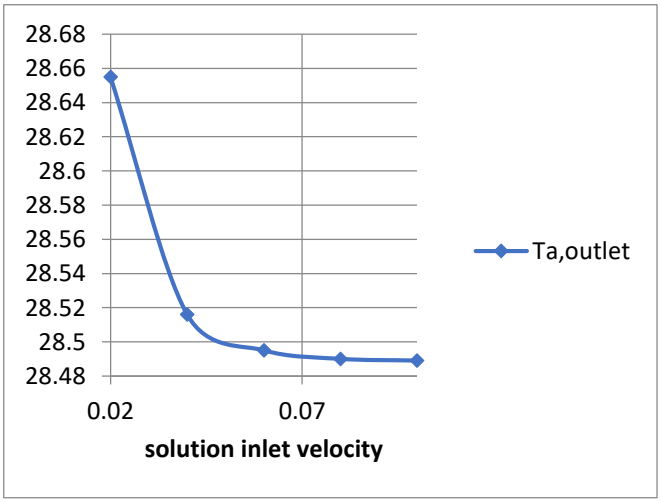

Figure8: Inlet velocity effect of the salt solution on the air outlet temperature (Ta,in= 25 °C , Ts,in= 35 °C , ωa,in= 10 g/kg , Cwat,in=80 % , Va,in= 0,1m/s)

Figure 9 shows the variation of the absolute humidity values of air at the outlet of the air channel as a

function of the solution flow velocity for velocities ranging between 0.01 m s^{-1} and 0.1 m s^{-1}. Also, we note a decrease of the outlet absolute humidity of air with increasing solution flow velocity.

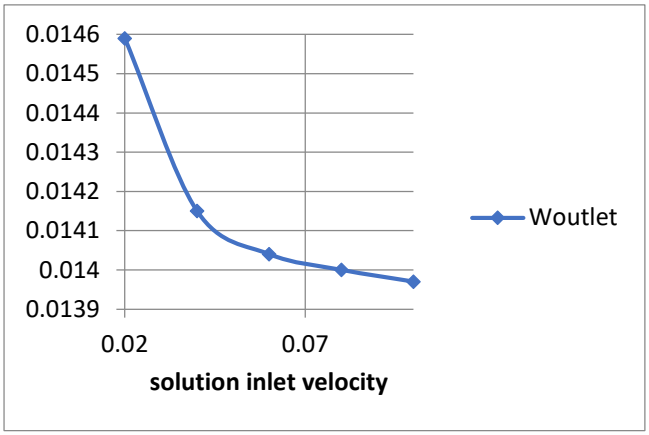

Figure9: Inlet velocity effect of the salt solution on the air outlet specific humidity (Ta,in= 25 °C , Ts,in= 35 °C , ωa,in= 10 g/kg , Cwat,in=80 % , Va,in= 0,1m/s)

Figure 10 shows the sensible and latent efficiencies for inlet air flow rates between 0.1 and 1 ms^{-1}. We remark that the sensible and latent efficiencies decrease with increasing the inlet air velocity. Also, the sensible efficiency is larger than the latent efficiency because mass resistance is always larger than thermal resistance for membrane processes.

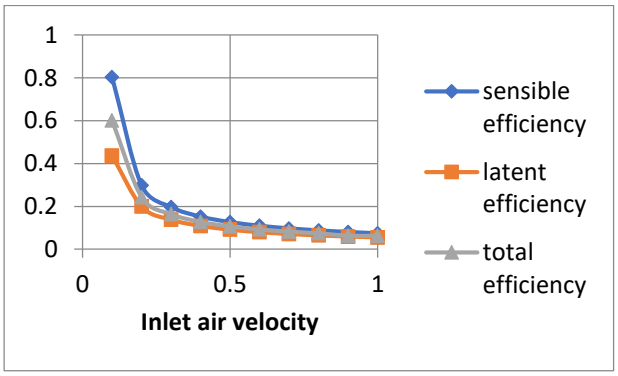

Figure10: Inlet velocity effect of the humid air on the sensible and latent efficiencies

(Ta,in= 25 °C , Ts,in= 35 °C , ωa,in= 10 g/kg , Cwat,in=80 % , Va,in= 0,1m/s)

The values of the two efficiencies are closer for relatively high velocity. These results are in agreement with those of Zhang [33].

5. CONCLUSION

The numerical results obtained by the suggested simulation are presented for different parameters. The temperature and mass profiles show that there is a coupled transfer of heat and mass which is a function of several parameters and boundary conditions. Increasing humid air flow rate decreases the residence time of the air in the exchanger which leads to a lower outlet air specific humidity and thus to a lower exchanger efficiency. The heat and mass exchange are ideal for relatively weak velocities. Also, we have noted that the humidification mass rate decreases with increasing air temperature and the air specific humidity increases with increasing inlet salt solution temperature.

6. ACKNOWLEDGEMENTS

The authors would like to express their gratitude to King Khalid University, Saudi Arabia for providing administrative and technical support.

REFERENCES

[1] E. Kabeel, M. H. Hamed Z. M. Omara and S. W. Sharshir, **"Water Desalination using a humidification-dehumidification technique-A Detailed Review**", (2013) Natural Resources, 4 pp. 286-305.

[2] G. O. Lof, **"Cooling with solar energy, congress on solar energy**",(1955) Tucson, AZ, pp. 171-189 .

[3] V. Oberg, D. Y. Goswami, **"Experimental study of the heat and mass transfer in a packed bed liquid desiccant air dehumidifier**", (1998) Journal of Solar Energy Engineering 120 pp. 289-297.

[4] H. M. Factor, G. Grossman, **"A packed bed dehumidifier/regenerator for solar air conditioning with liquid desiccants**", (1980) Solar Energy 24 pp. 541-550 .

[5] D. I. Stevens, J. E. Braun, S. A. Klein, **"An effectiveness model of liquid-desiccant system heat/mass exchangers**", (1980) Solar Energy 42 (6) pp. 449-455 .

[6] A. Y. Khan, **"Sensitivity analysis and component modelling of a packed-type liquid desiccant system at partial load operating conditions**", (1994) International Journal of Energy Research, 18 pp. 643-655 .

[7] A. Y. Khan and H. D. Ball, **"Development of a generalized model for performance evaluation of packed-type liquid sorbent dehumidifiers and regenerators**", (1992) ASHRAE Transactions 98 pp. 525-533 .

[8] N. Fumo, D. Y. Goswami, **"Study on an aqueous lithium chloride desiccant system: air dehumidification and desiccant regeneration**", (2002) Solar Energy, 72 pp. 351-361 .

[9] C. Ren, Y. Jiang, Y. Zhang, **"Simplified analysis of coupled heat and mass transfer processes in packed bed liquid desiccant-air contact system**", (2006) Solar Energy, 80 pp. 121-131.

[10] X.R. Zhang, L.Z. Zhang, H.M. Liu, L.X. Pei, **"One-step fabrication and analysis of an asymmetric cellulose acetate membrane for heat and moisture recovery**", (2011) Journal of Membrane. Sciences. 366 pp. 158–165.

[11] M. Gandiglio, A. Lanzini, M. Santarelli, P. Leone, **"Design and optimization of aproton exchange membrane fuel cell CHP system for residential use**", (2014) Energy Build. 69 pp. 381–393.

[12] D.G. Moghaddam, P. LePoudre, G. Ge, R.W. Besant, C.J. Simonson, **"Small-scale single-panel liquid-to-air membrane energy exchanger (LAMEE) test facility development, commissioning and evaluating the steady-state performance**", (2013) Energy and Buildings 66 pp. 424-436.

[13] D.G. Moghaddam, A. Oghabi, G. Ge, R.W. Besant, C.J. Simonson, **"Numerical model of small scale liquid to air**

membrane energy exchanger: Parametric study of membrane resistance and air side convective heat transfer coefficient", (2013) Applied Thermal Engineering 61 pp. 245-258.

[14] X.H. Ye, M.D. Levan, "**Water transport properties of nafion membranes. Part I.Single-tube membrane module for air drying**", (2003) J. Membr. Sci. 221 pp. 147–161.

[15] A.A. Al-Farayedhi, P. Gandhidasan, S.Y. Ahmed, "**Regeneration of liquiddesiccants using membrane technology**", (1999) Energy Convers. Manage. 40 pp 1405–1411.

[16] L. Dilandro, M. Pegoraro, L. Bordogna, "**Interaction of polyether-polyurethanewith water vapor and water-methane separation selectivity**", (1991) J. Membr. Sci. 64 pp. 229–236.

[17] P. Scovazzo, A. Hoehn, P. Todd, "**Membrane porosity and hydrophilicmembrane based dehumidification performance**", (2000) J. Membr. Sci. 167 pp. 217–225.

[18] P. Aranda, W.J. Chen, C.R. Martin, "**Water transport acrosspolystyrenesulfonate / alumina composite membranes**", (1995) J. Membr. Sci. 99 pp. 185–195.

[19] J. Min, J. Duan, "**Membrane-type total heat exchanger performance with heatand moisture transferring in different directions across membranes**", (2015) Appl.Therm. Eng. 91 pp. 1040–1047.

[20] P. Liu, M.R. Nasr, G. Ge, M.J. Alonso, H.M. Mathisen, F. Fathieh, C. Simonson, "**Atheoretical model to predict frosting limits in cross-flow air-to-air flat plateheat/energy exchangers**", (2016) Energy Build. 110 pp. 404–414.

[21] M. Afshin, "**Selection of the liquid desiccant in a run-around membrane energy exchanger**", (2010) Saskatoon, Saskatchewan, Canada: University of Saskatchewan.

[22] M. Seyed-ahmadi, B. Erb, C.J. Simonson, R.W. Besant, "**Transient behavior of runaround heat and moisture exchanger system, Part I: model formulation and verification**", (2009) International Journal of Heat and Mass Transfer, 52 pp. 6000-6011.

[23] S.M. Huang, L.Z. Zhang, K. Tang, L.X. Pei, "**Fluid flow and heat mass transfer in membrane parallel-plates channels used for liquid desiccant air dehumidification**", (2012) International Journal of Heat and Mass Transfer 55 pp. 2571-2580.

[24] H. Fan, C.J. Simonson, R.W. Besant, W. Shang, "**Performance of a run-around system for HVAC heat and moisture transfer applications using cross-flow plate exchangers coupled with aqueous lithium bromide**", (2006) HVAC&R Res 12 pp. 313-36.

[25] A.Q. Xiong, Y.J. Dai, R.Z. Wang, "**Development of a novel two-stage liquid desiccant dehumidification system assisted by CaCl2 solution using exergy analysis method**", (2010) Applied Energy 87 pp. 1495-1504.

[26] J.LNiu and L.Z Zhang, "**Membrane-based Enthalpy Exchanger: material considerations and clarification of moisture resistance**", (2001) Journal of Membrane Science, 189, 2 pp. 179-191.

[27] L.Z Zhang and J.LNiu, "**Effectiveness Correlations for Heat and Moisture Transfer Processes in an Enthalpy Exchanger with Membrane Cores**", (2002) Journal of Heat Transfer, 124 pp. 923.

[28] Li-Zhi Zhang, "**Heat and mass transfer in a cross-flow membrane-based enthalpy exchanger under naturally formed boundary conditions**", (2007) International Journal of Heat and Mass Transfer , 50, 1–2 pp. 151-162.

[29] M. Elimelech and W. A. Phillip, "**The Future of Seawater Desalination: Energy, Technology, and the Environment**", (2011), SCIENCE, 333 pp. 712-717.

[30] G. A. Longo, A. Gasparella, "**Experimental analysis on desiccant regeneration in a packed column with structured and random packing**", (2008) Solar Energy, 28 pp. 21-31.

[31] M. R. Conde, "**Properties of aqueous solutions of lithium and calcium chlorides: formulations for use in air conditioning equipment design**", (2004) International Journal of Thermal Sciences 43 pp. 367–382.

[32] S. V. Patankar, "**Numerical heat transfer and fluid flow**", (1980) Hemisphere publishing corporation, USA.

[33] L. H. Zhang, "**An Analytical solution to heat and mass transfer in hollow fiber membrane contactors for liquid desiccant air dehumidification**", (2011) Journal of Heat Transfer 133, pp. 1-8.